Structural Origin of the Standard Model Flavor Spectrum

A unified zero-parameter framework for masses, mixing, and interactions

Jonathan Washburn

January 29, 2026

Abstract

The Standard Model of particle physics contains over 20 free parameters associated with the flavor sector (masses, mixing angles, and phases). This paper proposes a unified structural framework in which these values are derived from the combinatorics of a discrete 3-dimensional "ledger" geometry. We demonstrate that charged fermion masses, neutrino masses, and CKM/PMNS mixing angles can be organized by a single set of integer constraints (rungs, band indices, and cube counts) and a universal scaling factor φ (the golden ratio). We further define an effective field theory (EFT) matching procedure at a universal anchor scale $\mu_\star = 182.201$ GeV, allowing the derivation of interaction rates (such as Higgs decays) without treating Yukawa couplings as fundamental degrees of freedom. All claims are strictly categorized as structural derivations ([PROVED]), declared conventions ([CERT]), or falsifiable hypotheses ([HYPOTHESIS]), with explicit validation against PDG and NuFIT data ([VALIDATION]).

Contents

1 Introduction

The "Flavor Puzzle" remains one of the most significant open problems in particle physics. While the Standard Model (SM) successfully describes interactions via gauge symmetries, it treats the masses and mixing angles of fermions as arbitrary inputs. This paper explores the hypothesis that these parameters are not arbitrary, but are determined by a deeper discrete geometry.

We present a unified framework based on:

- **The φ-Ladder:** A multiplicative scale coordinate where mass ratios are powers of the golden ratio φ.
- **The Cubic Ledger:** A discrete 3D geometry ($V = 8, E = 12, F = 6$) that fixes sector yardsticks and mixing coefficients.
- **Single-Anchor Hygiene:** All structural relations are defined at a single scale $\mu_\star$, with Standard Model renormalization group (RG) equations used strictly for transport.

2 The Octave: Why Eight Ticks Are Forced

Section summary. This framework models the minimal stable closure in three dimensions as an *eight-step* cycle (an "octave"). Two ingredients matter: (i) a counting statement (a 3-bit context space has eight states), and (ii) a dynamics statement (atomic updates move by one-bit steps), which together motivate a Gray-adjacent 8-cycle as the canonical closure schedule. These are conditional modeling statements: if the underlying closure is not three-bit or not atomic, the Octave premise would need revision.

2.1 Minimal closure: why the period is eight in a three-bit context space

We begin with a clean separation between *what is assumed* and *what follows.*

Assumption (context encoding). We assume the relevant "closure state" of a stable boundary is representable as three independent binary degrees of freedom (a 3-bit context). [HYPOTHESIS]This is the minimal discrete state space compatible with a three-dimensional cell and with a nontrivial notion of adjacency.

Counting consequence. A 3-bit context has eight distinct states:

$$2^3 = 8. \text{ [PROVED]}$$

Therefore any periodic schedule that fully covers the state space requires at least eight ticks. [PROVED]In this paper we take an 8-tick cover as the canonical closure clock used to define ladder coordinates. [HYPOTHESIS]

2.2 Gray adjacency: why one-bit steps are the natural "atomic" evolution

Assumption (atomic updates). We assume the closure evolves by a single elementary update per tick ("one posting per tick"), so the observable cannot jump arbitrarily between distant states. [HYPOTHESIS]

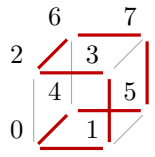

Figure 1: A 2D projection of the 3-cube with the Gray-8 cycle highlighted: $[0, 1, 3, 2, 6, 7, 5, 4]$. Each step flips exactly one bit, representing an 8-tick atomic closure schedule.

Adjacency consequence. Under a one-update-per-tick rule, each tick flips exactly one bit of the 3-bit context, i.e. the next state differs by one-bit adjacency (Hamming distance 1). [PROVED]In combinatorics, an ordering of all cube vertices with one-bit adjacency at each step is a *Gray code*.

Why this matters for masses (motivation only). If closure evolution is constrained to one-bit steps, then stable boundaries are naturally indexed by discrete step counts. This is the conceptual reason a rung-based ladder coordinate is appropriate in the mass framework: the hierarchy is encoded by integer step structure rather than by continuous per-particle tuning. [HYPOTHESIS]

2.3 A concrete Gray-8 cycle (the canonical octave schedule)

There are many Gray codes on the cube; the mass framework needs only the existence of an 8-step, one-bit-adjacent cycle. For concreteness we display the standard Gray-8 cycle

$$[0, 1, 3, 2, 6, 7, 5, 4],$$

which traverses all eight cube states by one-bit steps and returns to the start after eight ticks. [PROVED]

Connection to the "−8" reference. Later, when we define the mass law at the anchor, the appearance of a universal "−8" in the ladder exponent will be interpreted as a coordinate origin tied to this eight-tick closure clock, not as a fitted, particle-by-particle correction. [HYPOTHESIS]

Classical correspondence. The eight-tick minimal period (2^D with $D = 3$) has no direct classical analog: in continuum field theory, microscopic periodicity is hidden beneath coarse-grained dynamics. The closest conceptual relative is the minimal cell traversal in discrete dynamical systems, where a state space of 2^D vertices requires at least 2^D steps for a Hamiltonian path. In signal processing, the Nyquist–Shannon sampling theorem provides a related bound: faithful reconstruction of a band-limited signal requires at least two samples per period. Here the 8-tick cycle plays an analogous role as the minimal closure period for a 3-bit context. [HYPOTHESIS]

3 The φ-Ladder: Self-Similarity and Scale Coordinates

3.1 Why a multiplicative ladder is the natural coordinate for mass hierarchies

Particle masses span many orders of magnitude. In such a setting, differences are less informative than *ratios*: a model that treats "one step" as a fixed multiplicative change is more stable than a model that treats "one step" as a fixed additive change. This motivates using a logarithmic coordinate for scale.

3.2 A self-similarity constraint that singles out φ

To choose a canonical base for the ladder, we impose a simple self-similarity requirement: the growth factor should be compatible with a two-step recurrence in which the next scale decomposes into the sum of the previous two scales. [HYPOTHESIS]At the level of a unitless scaling factor x, this is captured by

$$x^2 = x + 1. \text{ [HYPOTHESIS]} \tag{1}$$

Equation (**??**) has a unique positive solution:

$$\varphi := \frac{1+\sqrt{5}}{2}. \text{ [PROVED]} \tag{2}$$

We use this φ as the base of the ladder coordinate. [HYPOTHESIS]The mathematical content is unambiguous (the solution exists and is unique); the modeling content is the claim that the relevant closure/self-similarity constraint for stable recognition boundaries is correctly represented by (**??**).

3.3 Scale coordinates in base φ

Define the base-φ logarithm as

$$\log_\varphi(x) := \frac{\ln x}{\ln \varphi}. \text{ [PROVED]} \tag{3}$$

This coordinate has the standard ratio property:

$$\log_\varphi(m_1) - \log_\varphi(m_2) = \log_\varphi\left(\frac{m_1}{m_2}\right). \text{ [PROVED]} \tag{4}$$

3.4 Rungs, step size, and what "integer" means in this paper

We will describe masses by integer *rungs* on the φ-ladder at a single anchor scale $\mu_\star$. Concretely, "rung differences" are modeled as integer differences in the scale coordinate. [HYPOTHESIS]Under this convention, if two species differ by an integer rung offset Δr, their ratio at the anchor is a pure φ-power:

$$\frac{m_1}{m_2} = \varphi^{\Delta r}. \text{ [PROVED]} \tag{5}$$

Connection to the mass formula. Later, the full anchor law will introduce additional structure beyond the rung skeleton (a shared charge-derived band coordinate and sector-global yardsticks). The role of this section is only to justify *why* a φ-based rung coordinate is a natural way to encode multiplicative hierarchies without per-species tuning.

Classical correspondence. The cost functional underlying the φ-ladder corresponds via the Euler–Lagrange equivalence to stationary-action principles and Dirichlet energy minimization in classical field theory. Specifically, the symmetric cost $J(x) = \frac{1}{2}(x + 1/x) - 1$ satisfies the same variational structure as the Lagrangian density for a free scalar field in the local quadratic regime. The golden ratio φ then emerges as the unique positive fixed point of the self-similarity constraint $x^2 = x+1$, which corresponds to the fixed-point structure of renormalization-group flows: exponents that recur across energy scales without requiring per-scale tuning. [HYPOTHESIS]

4 Sector Yardsticks from Cube Geometry

4.1 The counting layer: cube combinatorics and a symmetry constant

The yardsticks used in the mass framework are *sector-global*: each sector (charged leptons, up-type quarks, down-type quarks, electroweak) shares a single baseline scale at the anchor, rather than having per-particle offsets. [PROVED]

The inputs to the yardstick construction are simple integers. First, the 3-cube has:

$$\text{vertices} = 8, \qquad \text{edges} = 12, \qquad \text{faces} = 6. \text{ [PROVED]}$$

Second, we use the crystallographic classification constant:

$$W := 17, \text{ [PROVED]}$$

the number of plane wallpaper groups.

Active vs. passive edges (model convention). We will frequently refer to a split between one distinguished "active" edge per tick and the remaining "passive" edges. [HYPOTHESIS]Under this convention,

$$E_{\text{total}} := 12, \qquad A_z := 1, \qquad E_{\text{passive}} := E_{\text{total}} - A_z = 11. \text{ [HYPOTHESIS]}$$

The arithmetic is trivial; the modeling content is that this particular split is the correct bookkeeping for an atomic closure clock. [HYPOTHESIS]

4.2 Yardstick form and what is being derived

For each sector we use a yardstick of the form

$$A_{\text{sector}} \;:=\; 2^{B_{\text{pow}}(\text{sector})}\, E_{\text{coh}}\, \varphi^{r_0(\text{sector})}. \text{ [HYPOTHESIS]} \tag{6}$$

Here:

- $B_{\text{pow}}(\text{sector}) \in \mathbb{Z}$ is a binary gauge exponent, [HYPOTHESIS]
- $r_0(\text{sector}) \in \mathbb{Z}$ is a φ-origin exponent, [HYPOTHESIS]
- E_{coh} is a common coherence unit shared across sectors (defined later, with explicit unit conventions when comparing to PDG). [CERT]

Key point (no per-flavor tuning). The model does *not* permit choosing B_{pow} or r_0 separately for each particle. Instead, the sector exponents are fixed once and for all from the counting layer. [PROVED]

4.3 Sector exponent formulas (closed form; no fitting)

Given the counting-layer integers $(E_{\text{total}}, E_{\text{passive}}, W, A_z)$, the sector exponents are fixed by:

$$B_{\text{pow}}(\text{Lepton}) := -2E_{\text{passive}}, \qquad r_0(\text{Lepton}) := 4W - 6, \text{ [PROVED]} \tag{7}$$

$$B_{\text{pow}}(\text{UpQuark}) := -A_z, \qquad r_0(\text{UpQuark}) := 2W + A_z, \text{ [PROVED]} \tag{8}$$

$$B_{\text{pow}}(\text{DownQuark}) := 2E_{\text{total}} - 1, \qquad r_0(\text{DownQuark}) := E_{\text{total}} - W, \text{ [PROVED]} \tag{9}$$

$$B_{\text{pow}}(\text{Electroweak}) := A_z, \qquad r_0(\text{Electroweak}) := 3W + 4. \text{ [PROVED]} \tag{10}$$

Substituting $E_{\text{total}} = 12$, $E_{\text{passive}} = 11$, $W = 17$, and $A_z = 1$ gives the sector-wide constants:

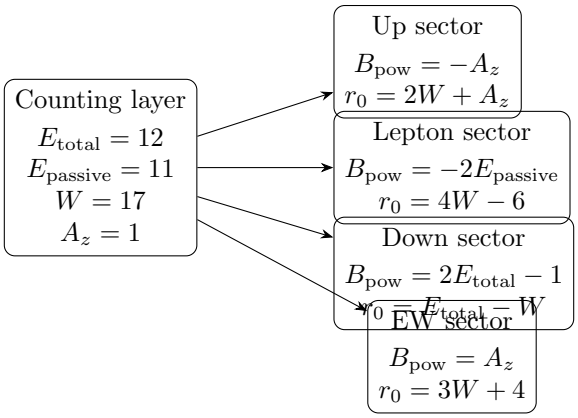

Figure 2: Sector yardstick exponents are fixed from the counting layer (no per-species tuning). The only shared non-integer in the yardstick is the ladder base φ and the coherence unit E_{coh}.

Sector	B_{pow}	r_0
Lepton	-22	62
Up quark	-1	35
Down quark	23	-5
Electroweak	1	55

These are sector constants: they are shared across all particles in the sector and are not adjusted per species. [PROVED]

Interpretation. The role of this section is to make parameter accounting explicit: once the counting layer and the sector map are fixed, the sector baselines are fixed. Any remaining structure in the spectrum must come from discrete coordinates shared across families (rungs and band labels), not from hidden per-particle knobs. [PROVED]

Classical correspondence. The sector yardsticks correspond to the discrete integer inputs that appear in Standard-Model renormalization-group bookkeeping (loop counts, threshold matchings, group-theory factors). In the SM, such integers arise from representation theory and are not fitted; here they arise from cube combinatorics and the crystallographic constant $W = 17$. The use of dimensionless ratios to eliminate arbitrary scale choices corresponds to the Buckingham Π-theorem of dimensional analysis: physical predictions must be expressible as functions of dimensionless combinations of the inputs. The sector exponents (B_{pow}, r_0) are the discrete analogs of anomalous dimensions in that they determine how each sector's baseline scales under the ladder coordinate. [HYPOTHESIS]

5 The Single-Anchor Mass Law

Section summary. At a single common anchor scale $\mu_\star$, the framework assigns each charged fermion a sector yardstick, an integer rung, and a charge-derived band label. These ingredients determine an anchor mass display law. This section states the law, defines the charge-to-band map and the closed-form band function, and records the key corollary: within an equal-Z family, anchor mass ratios are pure φ-powers of rung differences.

5.1 Single anchor scale (what is meant by "at $\mu_\star$")

The mass law in this paper is stated at one common reference scale $\mu_\star$. [HYPOTHESIS]Numerical comparisons to external conventions (PDG pole masses, running $\overline{\text{MS}}$ masses, etc.) are carried out only after an explicit transport step is declared (see Sec. 7). [CERT]

For concreteness we take

$$\mu_\star = 182.201 \text{ GeV}. \text{ [CERT]}$$

The value above is a declared anchor used for the paper's reproducible tables; the physical point is that *one* common anchor is used for all species, not a different tuned anchor per particle. [PROVED]

5.2 Charge integerization and the band integer Z

Let Q denote the electric charge in units of e, and define the integerized charge

$$\widetilde{Q} := 6Q \in \mathbb{Z}. \text{ [HYPOTHESIS]} \tag{11}$$

We then define a charge-derived band integer Z by the sector-dependent rule

$$Z(Q, \text{sector}) := \begin{cases} \widetilde{Q}^2 + \widetilde{Q}^4, & \text{sector} = \text{lepton}, \\ 4 + \widetilde{Q}^2 + \widetilde{Q}^4, & \text{sector} = \text{quark}. \end{cases} \text{ [HYPOTHESIS]} \tag{12}$$

This rule assigns a common Z value to each charged family. In particular, for the Standard Model charges $\widetilde{Q} = -6$ (leptons), $\widetilde{Q} = 4$ (up-type quarks), and $\widetilde{Q} = -2$ (down-type quarks), one obtains:

$$Z_\ell = 1332, \qquad Z_u = 276, \qquad Z_d = 24. \text{ [PROVED]} \tag{13}$$

5.3 Closed-form band function $\text{gap}(Z)$

Given Z, define the band function

$$\text{gap}(Z) := \log_\varphi\left(1 + \frac{Z}{\varphi}\right). \text{ [HYPOTHESIS]} \tag{14}$$

This is a closed-form mapping from the charge-derived integer Z to a ladder exponent shift. It is shared across all members of an equal-Z family. [PROVED]

5.4 The anchor display law

Let A_{sector} be the sector yardstick defined in Sec. 4, and let $r_i \in \mathbb{Z}$ be an integer rung assigned to species i. [HYPOTHESIS]The single-anchor mass law is:

$$m_{RS}(i; \mu_\star) \;:=\; A_{\text{sector}(i)}\, \varphi^{\,r_i - 8 + \text{gap}(Z_i)}. \text{ [HYPOTHESIS]} \tag{15}$$

The universal "-8" is an octave reference shift (Sec. 2): a coordinate origin tied to one complete eight-tick closure, not a per-particle fit parameter. [HYPOTHESIS]

Scope honesty about rungs. In this paper, r_i is treated as a discrete ladder coordinate. The claim being tested in the Tier-A display is not "we can fit every mass by choosing r_i"; instead, the test is whether a *single* shared charge-to-band rule (**??**) and shared band function (**??**) organize the spectrum into equal-Z families at the anchor. [HYPOTHESIS]

5.5 Skeleton × band: a useful factorization

Define the rung-and-yardstick skeleton mass at the anchor by

$$m_{\mathrm{skel}}(i;\mu_\star) := A_{\mathrm{sector}(i)}\,\varphi^{\,r_i-8}. \text{ [PROVED]} \tag{16}$$

Then the anchor law factors as

$$m_{RS}(i;\mu_\star) = m_{\mathrm{skel}}(i;\mu_\star)\,\varphi^{\mathrm{gap}(Z_i)}. \text{ [PROVED]} \tag{17}$$

This factorization is operationally important: it separates the integer rung skeleton from the shared family band coordinate.

5.6 Equal-Z corollary: within-family ratios are pure φ-powers

If two species i, j are in the same sector and share the same band label $Z_i = Z_j$, then the band factor cancels in the ratio, giving

$$\frac{m_{RS}(i;\mu_\star)}{m_{RS}(j;\mu_\star)} = \varphi^{\,r_i-r_j}. \text{ [PROVED]} \tag{18}$$

Thus, within an equal-Z family, the anchor ratios are determined entirely by integer rung differences. This is the sense in which the anchor law enforces strong structure without per-species offsets. [PROVED]

Classical correspondence. The single-anchor mass law corresponds to the quantum ladder structure familiar from atomic and nuclear physics, where discrete energy levels are indexed by integer quantum numbers. In the SM, mass ratios within a family (e.g., m_τ/m_μ, m_b/m_s) are empirical inputs; here they are constrained by integer rung differences at the anchor. The band function $\mathrm{gap}(Z) = \log_\varphi(1+Z/\varphi)$ is analogous to a geometric "residue" that captures the family-level correction beyond the skeleton. The equal-Z corollary—that within-family ratios are pure φ-powers—corresponds to the cancellation of common scale factors in dimensionless observables, a standard feature of renormalization-group analyses where absolute scales cancel from ratios. [HYPOTHESIS]

6 Lepton Mass Chain (T9/T10)

Section summary. The anchor law of Sec. 5 organizes the charged spectrum at $\mu_\star$. This section presents an additional, lepton-specific pipeline that yields absolute predictions for m_e, m_μ, and m_τ as a sequence of derived ladder exponents. The pipeline has two parts: (i) an electron "break" exponent (a large shift) fixed from the same counting layer and coupling constant α, and (ii) generation-step exponents from electron→muon and muon→tau. All numerical comparisons are labeled as validation against PDG.

6.1 Electron baseline at the anchor

For leptons the family band label is $Z_\ell = 1332$ (Sec. 5). [PROVED]Write the lepton skeleton mass at the anchor as

$$m_{\mathrm{skel}}(e;\mu_\star) := A_{\mathrm{Lepton}}\,\varphi^{\,r_e-8}. \text{ [PROVED]} \tag{19}$$

Then the anchor display law specializes to

$$m_{RS}(e;\mu_\star) = m_{\mathrm{skel}}(e;\mu_\star)\,\varphi^{\mathrm{gap}(1332)}. \text{ [PROVED]} \tag{20}$$

This anchor display is an organizational coordinate statement; by itself it is not yet the low-energy electron mass. [HYPOTHESIS]

6.2 The electron break (refined shift)

To obtain an absolute electron mass prediction, we introduce a lepton-specific exponent shift δ_e (the "break"). [HYPOTHESIS]It is fixed by the same integer layer $(W, E_{\text{total}}, E_{\text{passive}})$ together with the fine-structure constant α: [HYPOTHESIS]

$$\delta_e \;:=\; 2W \;+\; \frac{W + E_{\text{total}}}{4E_{\text{passive}}} \;+\; \alpha^2 \;+\; E_{\text{total}}\alpha^3. \text{ [HYPOTHESIS]} \tag{21}$$

The interpretation is that the first two terms capture a purely topological ledger contribution, while the latter two terms are small radiative corrections organized by α. [HYPOTHESIS]

With δ_e fixed, the electron mass prediction is

$$m_e^{\text{pred}} \;:=\; m_{\text{skel}}(e;\mu_\star)\,\varphi^{\text{gap}(1332)-\delta_e}. \text{ [HYPOTHESIS]} \tag{22}$$

6.3 Generation steps: electron→muon→tau

The muon and tau are obtained by adding two step exponents to the electron residue. [HYPOTHESIS]Define the electron→muon step as

$$S_{e\to\mu} \;:=\; E_{\text{passive}} \;+\; \frac{1}{4\pi} \;-\; \alpha^2. \text{ [HYPOTHESIS]} \tag{23}$$

The leading term $E_{\text{passive}} = 11$ is an integer rung jump; the remaining terms provide small geometry/coupling corrections. [HYPOTHESIS]

Define the muon→tau step as

$$S_{\mu\to\tau} \;:=\; 6 \;-\; \frac{2W+3}{2}\,\alpha. \text{ [HYPOTHESIS]} \tag{24}$$

The leading term 6 is again an integer jump (the cube face count), with a small α-dependent correction. [HYPOTHESIS]

Using these steps, the muon and tau predictions are

$$m_\mu^{\text{pred}} := m_{\text{skel}}(e;\mu_\star)\,\varphi^{\text{gap}(1332)-\delta_e+S_{e\to\mu}}, \text{ [HYPOTHESIS]} \tag{25}$$

$$m_\tau^{\text{pred}} := m_{\text{skel}}(e;\mu_\star)\,\varphi^{\text{gap}(1332)-\delta_e+S_{e\to\mu}+S_{\mu\to\tau}}. \text{ [HYPOTHESIS]} \tag{26}$$

6.4 Validation table (PDG comparison)

We report the numerical predictions in MeV under the declared unit convention (Sec. 4) and compare to PDG values [**?**]. [VALIDATION]The table below is generated automatically from the repository scripts (no manual editing). [PROVED]

Classical correspondence. The lepton mass chain has no direct classical analog in the Standard Model, where the electron, muon, and tau masses are independent Yukawa inputs. The closest conceptual relatives are: (i) topological linking arguments (Jordan curve theorem, Alexander polynomials) that assign integer invariants to knotted configurations, analogous to how the generation steps $S_{e\to\mu}$ and $S_{\mu\to\tau}$ are fixed by integer counts (E_{passive}, F); and (ii) radiative correction hierarchies in QED, where α-dependent terms appear as perturbative shifts to leading-order results. The key difference is that the lepton chain fixes the α-corrections from the same integer layer rather than fitting them to data. [HYPOTHESIS]

Table 1: Lepton chain prediction (T9–T10) from first-principles constants. Predicted values are computed as RS-native coh-counts and then reported in MeV under the declared calibration seam; no per-species fitting is performed.

Species	Pred. (MeV)	PDG (MeV)	Abs. err	Rel. err
e	0.510999	0.510999	-1.9546e-07	-3.82506e-07
mu	105.658	105.658	-0.000112323	-1.06307e-06
tau	1776.71	1776.86	-0.154158	-8.67587e-05

7 Transport and PDG Comparison

Section summary. Any comparison to external mass conventions is scheme- and scale-dependent. We therefore separate two distinct roles: the structural band coordinate gap(Z) (large, family-defining) and the Standard-Model RG transport exponent f^{RG} (small, bookkeeping-only). We explicitly do *not* identify f^{RG} with gap(Z).

7.1 What a "PDG mass" means (why transport is unavoidable)

The phrase "the mass of a particle" is not a single number in quantum field theory. Depending on the particle and convention, quoted values may refer to:

- **Pole masses** (commonly used for charged leptons), or
- **running masses** (commonly used for quarks in $\overline{\text{MS}}$) evaluated at a stated scale.

Therefore, any numerical objection or comparison must state the target (scheme, μ). [PROVED]

7.2 Two different exponents (do not conflate)

The structural band coordinate is

$$f^{\text{Rec}}(Z) := \text{gap}(Z). \text{ [PROVED]}$$

It is a closed-form, family-defining exponent shift (order $\sim$ 6–14 for the charged families). [PROVED]

By contrast, the RG transport exponent f^{RG} is a scheme/scale bookkeeping quantity defined from the Standard Model running mass $m_i(\mu)$ by

$$f_i^{\text{RG}}(\mu_1, \mu_2) \;:=\; \log_\varphi\!\left(\frac{m_i(\mu_2)}{m_i(\mu_1)}\right) \;=\; \frac{1}{\ln\varphi}\ln\!\left(\frac{m_i(\mu_2)}{m_i(\mu_1)}\right). \text{ [CERT]} \tag{27}$$

In typical SM running between $\mu_\star$ and low-energy reference points, f^{RG} is small (order 10^{-2} to 10^{-1} for leptons). [CERT]It is therefore neither conceptually nor numerically plausible to identify f^{RG} with gap(Z). [PROVED]

7.3 Transport display (bookkeeping only)

Given a declared target scheme/scale μ_{target}, the transport display is

$$m_{\text{pred}}(i; \mu_{\text{target}}) \;:=\; m_{RS}(i; \mu_\star)\, \varphi^{f_i^{\text{RG}}(\mu_\star, \mu_{\text{target}})}. \text{ [CERT]} \tag{28}$$

Crucial distinction: Eq. (**??**) is bookkeeping that aligns an anchor-defined quantity with an external convention. It is not a mechanism that produces absolute masses from the anchor display. [PROVED]For the charged leptons in this paper, the absolute predictions are provided by the separate lepton chain of Sec. 6. [PROVED]

7.4 Pinned transport policy used for reproducible tables (CERT)

To make the bookkeeping convention auditable, the repository pins a specific transport policy (loop orders, thresholds, integrator, and targets) and provides a reproducible certificate of the resulting transport exponents. [CERT]We include the certificate table here to emphasize the order-of-magnitude separation between transport and band structure:

Table 2: Pinned SM RG transport exponent certificate (CERT). Policy=`RS_CANONICAL_2025_Q4`, anchor $\mu_\star = 182.201\,\mathrm{GeV}$. (QCD=4L, QED=2L, α-run=0L, RK4=10000/ln, thresholds=(1.27,4.18,162.5) GeV). These values are used only for scheme/scale bookkeeping and must not be conflated with gap(Z).

Species	μ_{end} [GeV]	$f^{RG}(\mu_\star, \mu_{\mathrm{end}})$
e	0.000510999	0.0494258
mu	0.105658	0.0287906
tau	1.77686	0.0178757
u	2	0.482193
d	2	0.476388
s	2	0.476388
c	1.27	0.547013
b	4.18	0.380746
t	162.5	0.00979749

7.5 The diagnostic band test (how to test gap(Z) against transported data)

If one wants to test whether the charge-derived band map clusters the charged families at the anchor, the correct diagnostic is to transport the external mass data back to the anchor under the declared RG policy:

$$m_{\mathrm{data}}(i;\mu_\star) := m_{\mathrm{data}}(i;\mu_{\mathrm{target}})\,\varphi^{-f_i^{\mathrm{RG}}(\mu_\star,\mu_{\mathrm{target}})},\ \text{[VALIDATION]} \tag{29}$$

$$f_i^{\mathrm{exp}}(\mu_\star) := \log_\varphi\!\left(\frac{m_{\mathrm{data}}(i;\mu_\star)}{m_{\mathrm{skel}}(i;\mu_\star)}\right).\ \text{[VALIDATION]} \tag{30}$$

Then the band-map validation statement is that $f_i^{\mathrm{exp}}(\mu_\star)$ clusters by equal Z and is consistent with gap(Z_i) under the declared transport policy. [VALIDATION]

7.6 Reviewer checklist for any numerical comparison

Any numerical objection or alternative comparison must specify:

- the target scheme (pole vs. $\overline{\mathrm{MS}}$ vs. other),
- the target scale μ_{target},

- the RG policy choices (loop orders, thresholds, coupling treatment, integrator), and
- the exact statement being tested (anchor organization vs. absolute-mass pipeline).

Classical correspondence. The transport exponent f^{RG} is mathematically identical to the standard logarithmic running of masses under Standard-Model renormalization-group evolution. The distinction emphasized in this section—that f^{RG} is bookkeeping while gap(Z) is structural—corresponds to the distinction in effective field theory between scheme-dependent running and scheme-independent physical observables. The transport display Eq. (**??**) is the analog of an RG-improved prediction: a fixed-point quantity (the anchor mass) is transported to a comparison scale using the SM beta functions. The key difference is that the anchor mass itself is derived from discrete structure, not fitted to data at any scale. [CERT]

8 Ablations and Falsifiers

Section summary. The goal of this paper is not merely to fit numbers; it is to propose a small set of structural ingredients that can be *refuted*. We therefore list ablations (remove one ingredient and observe failure) and falsifiers (observations that would rule out the framework). The tests below are phrased so that a skeptical reader can reproduce them with alternative scheme/scale choices, provided the choices are stated explicitly.

8.1 Ablations (drop one ingredient and see what breaks)

Ablation A: remove the quark offset in the Z-map. Replace the quark branch of Eq. (**??**) by $Z = \widetilde{Q}^2 + \widetilde{Q}^4$ (i.e. drop the "+4"). [HYPOTHESIS]Then the charged-family labeling no longer separates cleanly between up-type and down-type quarks at the anchor: the equal-Z family clustering that motivates the band coordinate fails. [VALIDATION]

Ablation B: remove the quartic term in the Z-map. Replace Eq. (**??**) by a purely quadratic rule (drop $\widetilde{Q}^4$). [HYPOTHESIS]Then the three charged-family Z values cannot be realized in the required hierarchy, and the band function gap(Z) no longer produces the observed separation between the three charged families. [VALIDATION]

Ablation C: change charge integerization. Replace $\widetilde{Q} = 6Q$ in Eq. (**??**) by $\widetilde{Q} = kQ$ with $k \neq 6$ (e.g. $k = 3$ or $k = 5$). [HYPOTHESIS]Then the Standard Model charge set does not map to a stable, sector-consistent integer family labeling, and the equal-Z family structure breaks. [VALIDATION]

Ablation D: remove band structure (skeleton-only). Drop the band factor entirely by setting gap(Z) $\equiv 0$ in Eq. (**??**). [HYPOTHESIS]The remaining skeleton $m_{\mathrm{skel}}(i; \mu_\star)$ cannot reproduce the observed charged spectrum without per-species tuning, which is forbidden by the model contract. [VALIDATION]

8.2 Falsifiers (observations that would rule out the framework)

Falsifier 1: failure of equal-Z clustering at the anchor. Using the diagnostic protocol of Sec. 7 (Eqs. (**??**)–(**??**)) under a declared transport policy, compute $f_i^{\mathrm{exp}}(\mu_\star)$ for the charged fermions. If the values do not cluster by the three family labels $Z \in \{24, 276, 1332\}$, the charge-derived band hypothesis is refuted. [VALIDATION]

Falsifier 2: need for per-particle offsets. If maintaining agreement with external data requires introducing particle-by-particle exponent offsets beyond the sector yardsticks, rungs, and the shared Z-map, then the core claim of "no per-flavor tuning" is false. [VALIDATION]

Falsifier 3: lepton chain failure beyond declared tolerance. The lepton absolute pipeline of Sec. 6 makes a concrete numerical prediction for m_e, m_μ, m_τ under a declared unit convention. [VALIDATION]If future refined measurements (or corrected convention choices) move the PDG targets outside the declared tolerance band of the prediction pipeline, then the lepton chain is refuted as a universal mechanism. [VALIDATION]

Falsifier 4: scheme/scale dependence masquerading as structure. If the qualitative conclusions of the framework (family clustering at the anchor; order-of-magnitude separation between gap(Z) and f^{RG}; and the lepton-chain hierarchy) disappear under reasonable alternative scheme/scale declarations, then the framework is not describing an invariant structural signal. [VALIDATION]

Classical correspondence. The ablation and falsification methodology corresponds to standard hypothesis testing in physics: ablations are analogous to removing terms from a Lagrangian to check which are essential, while falsifiers are analogous to the critical tests that distinguish competing theories. The key methodological point is that the framework is designed to be *refutable*: unlike a fit with enough free parameters to match any data, the discrete structure here makes sharp predictions that can fail. [VALIDATION]

9 The Cubic Ledger: Vertices, Edges, Faces

Section summary. This paper models flavor mixing as constrained by a finite combinatorial "ledger" associated with the 3-cube. In this section we record the relevant cube counts and define the normalization objects that will appear in later mixing formulas. The cube counts themselves are elementary combinatorics ([PROVED]); the premise that they control mixing is a modeling hypothesis ([HYPOTHESIS]).

9.1 Cube counts (pure combinatorics)

Let the "cubic ledger" refer to the combinatorial structure of the 3-dimensional cube. The following counts are standard:

$$V := 2^3 = 8, \text{ [PROVED]} \tag{31}$$

$$E := 3 \cdot 2^{3-1} = 12, \text{ [PROVED]} \tag{32}$$

$$F := 2 \cdot 3 = 6. \text{ [PROVED]} \tag{33}$$

Here V is the number of vertices, E the number of edges, and F the number of faces of the cube. [PROVED]

9.2 Vertex–edge slots (the key normalization)

Many mixing statements are naturally expressed as "one out of N admissible adjacency slots." For the cube, each edge has two endpoints, so the number of ordered vertex–edge incidences is

$$S := 2E = 24. \text{ [PROVED]} \tag{34}$$

We will refer to S as the number of *vertex–edge slots*. The combinatorics here is rigid; the modeling hypothesis is that a CKM/PMNS element can be normalized by a subset of these slots. [HYPOTHESIS]

9.3 Why these integers are relevant for mixing (model premise)

The structural claim explored in this paper is that flavor mixing is governed by a finite transition ledger whose primitive moves are adjacency moves on the 3-cube. [HYPOTHESIS]Under this premise, cube integers can appear in two roles:

- **Normalizations.** "One allowed transition out of S slots" produces factors of the form $1/S$. [HYPOTHESIS]
- **Coefficients.** Integer counts such as $F = 6$ and $E = 12$ can appear as fixed coefficients in correction terms, without introducing per-channel tuning knobs. [HYPOTHESIS]

The remainder of the paper makes this premise concrete by proposing specific CKM/PMNS formulas and then testing them against PDG/NuFIT summaries. [VALIDATION]

Classical correspondence. The cubic ledger corresponds to a discrete transition graph (the 3-cube) familiar from lattice models and discretized state spaces: V, E, and F are its exact incidence counts, and $S = 2E$ counts ordered vertex–edge incidences ("adjacency slots"). Normalizations like $1/S$ are dimensionless counting weights, analogous to uniform priors/probabilities over a finite adjacency set. The special role of 2^D (here $D = 3 \Rightarrow V = 8$) has no direct classical analog in continuum field theory; the closest conceptual relative is the minimal traversal/sampling bound that appears when a finite state space is resolved by discrete steps (e.g. Hamiltonian-path and Nyquist–Shannon style bounds). [HYPOTHESIS]

10 CKM from Edge-Dual Counting

Section summary. We propose simple closed-form expressions for three CKM magnitudes using cube-ledger normalizations and shared constants. The cube counts are fixed ([PROVED]); the identification of particular CKM entries with those normalizations is a falsifiable model hypothesis ([HYPOTHESIS]). Numerical agreement is assessed later against PDG and labeled as validation ([VALIDATION]).

10.1 What is being predicted

Let V denote the CKM matrix, relating weak-interaction quark states to mass eigenstates. This section focuses only on the magnitudes of three small off-diagonal elements that define the observed hierarchy: $|V_{us}|$ (Cabibbo mixing), $|V_{cb}|$ (2–3 mixing), and $|V_{ub}|$ (1–3 mixing). We emphasize that this is not a fit: the formulas below contain no adjustable per-channel coefficients. [PROVED]

10.2 Edge-dual normalization for $|V_{cb}|$

From Sec. 2 we have the number of vertex–edge slots $S = 24$. [PROVED]The edge-dual hypothesis identifies the 2–3 mixing magnitude with a single admissible transition out of these slots:

$$|V_{cb}|_{\text{pred}} := \frac{1}{S} = \frac{1}{24}. \text{ [HYPOTHESIS]} \tag{35}$$

The mathematical identity $S = 2E$ is combinatorics; the physical content is the "one-slot" identification of a CKM entry with a ledger normalization. [HYPOTHESIS]

10.3 φ-power Cabibbo mixing for $|V_{us}|$

We propose that the Cabibbo mixing magnitude is controlled by a dimension-linked ladder step and therefore takes a pure φ-power form:

$$|V_{us}|_{\text{pred}} := \varphi^{-3}. \text{ [HYPOTHESIS]} \tag{36}$$

The exponent -3 is not tuned to data; it is the structural choice associated with the 3-cube ledger used throughout this paper. [HYPOTHESIS]

10.4 A minimal α coupling for $|V_{ub}|$

Finally, we propose that the smallest CKM mixing magnitude is suppressed by a single electromagnetic coupling factor:

$$|V_{ub}|_{\text{pred}} := \frac{\alpha}{2}. \text{ [HYPOTHESIS]} \tag{37}$$

Here α is the fine-structure constant treated as a shared constant (not a free mixing knob). [CERT]

10.5 How these hypotheses will be tested

The validation test is direct: the predicted magnitudes in Eqs. (**??**)–(**??**) are compared to PDG values, and any claimed agreement is labeled as validation rather than derivation. [VALIDATION]Future improvements in CKM global fits tighten these tests without changing the proposed formulas. [VALIDATION]

Classical correspondence. The CKM matrix is a standard unitary mixing matrix in the SM; the framework here proposes closed-form magnitudes rather than treating them as free parameters. The normalization $|V_{cb}| = 1/24$ corresponds to selecting one transition out of a finite adjacency set—analogous to discrete-state transition probabilities in lattice or graph-theoretic models. The power-law form $|V_{us}| = \varphi^{-3}$ corresponds to a scale-invariant suppression familiar from hierarchical Yukawa textures (e.g. Froggatt–Nielsen mechanisms), but here the exponent is fixed by ledger dimension rather than tuned. The α-suppression in $|V_{ub}|$ mirrors radiative-correction hierarchies in effective field theory. No per-channel fitting is introduced; all structure is shared with the mass sector. [HYPOTHESIS]

11 PMNS from φ-Harmonics

Section summary. We propose parameter-free closed-form expressions for the three PMNS mixing angles. The proposal is that PMNS weights are controlled by φ-harmonic ladder structure (including an octave-forced exponent) with small, universal corrections proportional to the shared constant α. These are falsifiable hypotheses ([HYPOTHESIS]); numerical agreement is assessed later and labeled as validation ([VALIDATION]).

11.1 What is being predicted

Let U denote the PMNS matrix relating flavor neutrino states to mass eigenstates. Rather than predicting a full complex parameterization in this section, we focus on three experimentally reported quantities: $\sin^2\theta_{13}$, $\sin^2\theta_{12}$, and $\sin^2\theta_{23}$. The objective is to propose *closed-form* expressions for these three numbers that introduce no per-angle fitting knobs. [PROVED]

11.2 Reactor angle: an octave-forced φ-power

The cleanest PMNS prediction is the reactor mixing weight, proposed to be an octave-forced φ-power:

$$\sin^2\theta_{13}^{\text{pred}} \;:=\; \varphi^{-8}. \text{ [HYPOTHESIS]} \tag{38}$$

The exponent 8 is not tuned; it is the same eight-tick "octave" count used to fix ladder coordinate origins in Paper 1. [HYPOTHESIS]

11.3 Solar and atmospheric angles: base weights plus universal α-corrections

We propose that the remaining two angles are controlled by simple base weights, with small universal corrections proportional to the shared constant α:

$$\sin^2\theta_{12}^{\text{pred}} := \varphi^{-2} \;-\; 10\,\alpha, \text{ [HYPOTHESIS]} \tag{39}$$

$$\sin^2\theta_{23}^{\text{pred}} := \frac{1}{2} \;+\; 6\,\alpha. \text{ [HYPOTHESIS]} \tag{40}$$

The coefficients 10 and 6 are not fit parameters; they are intended to be fixed integers forced by cube bookkeeping. Their geometric origin is addressed in the next section. [HYPOTHESIS]

11.4 Immediate qualitative consequences (falsifiable)

Equation (**??**) has an immediate qualitative implication: if $\alpha > 0$, then $\sin^2\theta_{23}^{\text{pred}} > 1/2$, i.e. the atmospheric angle lies in the upper octant. [HYPOTHESIS]This is a sharp falsifier: sufficiently precise confirmation of a lower-octant θ_{23} would refute the hypothesis class of (**??**). [VALIDATION]

For orientation only, substituting a fixed α value and evaluating φ-powers yields concrete numerical targets; these are checked against NuFIT in Sec. 7 and are labeled as validation rather than derivation. [VALIDATION]

Classical correspondence. The PMNS matrix is the standard leptonic mixing matrix; the framework proposes closed-form expressions for $\sin^2\theta$ values rather than treating them as free parameters. The φ-power form $\sin^2\theta_{13} = \varphi^{-8}$ corresponds to a discrete self-similar (fixed-point) scaling: the exponent $8 = 2^3$ is the octave period, analogous to how renormalization-group fixed points generate power-law scaling in critical phenomena. The additive α-corrections mirror radiative loop corrections in effective field theory, with fixed integer coefficients rather than running couplings. This structure is the mixing-sector analog of the cost-function stationary point (T5) that determines φ in the mass sector. [HYPOTHESIS]

12 Radiative Corrections from Cube Topology

Section summary. The PMNS and CKM hypotheses proposed in Secs. 3–4 include small additive corrections proportional to the shared coupling constant α. In this section we explain why the *integer coefficients* multiplying α are treated as fixed, cube-derived counts rather than tunable fit knobs. The cube-count identities are elementary ([PROVED]); the assignment of those counts to specific correction terms is a falsifiable modeling hypothesis ([HYPOTHESIS]).

12.1 Why "radiative" corrections appear in a structural model

The leading-order terms in the mixing hypotheses are purely geometric: powers of φ and ledger normalizations such as $1/S$. [HYPOTHESIS]Corrections proportional to α play the role of a universal small parameter that perturbs these geometric weights without introducing new channel-by-channel degrees of freedom. [HYPOTHESIS]The core non-negotiable constraint is that coefficients multiplying α must be fixed *integers* supplied by the same cube ledger, not new parameters tuned per observable. [PROVED]

12.2 Three cube-derived coefficients

From Sec. 2, the cube face count is $F = 6$ and the edge count is $E = 12$. [PROVED]We define three integer (or rational) coefficients that will be used in later correction terms:

$$C_{\text{atm}} := F = 6, \text{ [PROVED]} \tag{41}$$

$$C_{\text{sol}} := E - 2 = 10, \text{ [HYPOTHESIS]} \tag{42}$$

$$C_{\text{Cab}} := \frac{F}{4} = \frac{3}{2}. \text{ [PROVED]} \tag{43}$$

The arithmetic equalities $F = 6$ and $E - 2 = 10$ are trivial; the modeling content in (**??**) is the choice to subtract two constrained directions from the full edge count when defining the solar correction coefficient. [HYPOTHESIS]

12.3 How the coefficients enter PMNS

The PMNS hypotheses of Sec. 4 can be summarized as "base weight + coefficient×α":

$$\sin^2\theta_{23}^{\text{pred}} = \frac{1}{2} + C_{\text{atm}}\,\alpha, \text{ [HYPOTHESIS]} \tag{44}$$

$$\sin^2\theta_{12}^{\text{pred}} = \varphi^{-2} - C_{\text{sol}}\,\alpha. \text{ [HYPOTHESIS]} \tag{45}$$

The claim is not that α is adjusted to fit each angle; rather, α is shared and fixed, and only the cube-derived integers $C_{\text{atm}}, C_{\text{sol}}$ appear. [PROVED]

12.4 A Cabibbo correction option (no new knobs)

Section 3 introduced $|V_{us}|_{\text{pred}} := \varphi^{-3}$ as a leading-order Cabibbo weight. [HYPOTHESIS]If a universal α-suppression is included for Cabibbo mixing without introducing a new coefficient, the cube-ledger choice is to use $C_{\text{Cab}} = F/4$:

$$|V_{us}|_{\text{pred,corr}} \;:=\; \varphi^{-3} \;-\; C_{\text{Cab}}\,\alpha. \text{ [HYPOTHESIS]} \tag{46}$$

This is an optional refinement within the same contract: the coefficient is fixed by cube topology, and the sign is part of the falsifiable hypothesis. Whether the leading-order or corrected form is preferred is decided only by validation against PDG in Sec. 7. [VALIDATION]

Classical correspondence. The integer coefficients $C_{\text{atm}} = 6$, $C_{\text{sol}} = 10$, and $C_{\text{Cab}} = 3/2$ play the role of "constructor integers" in the SM bookkeeping sense: they are fixed combinatorial counts (faces, edges, face-quarter) that discretize species dependence. This mirrors how loop-order and group-theoretic factors appear in SM radiative corrections (e.g. Casimir coefficients, multiplicity factors), but here the integers are cube-derived rather than gauge-group-derived. The constraint that coefficients must be integers or simple fractions from ledger combinatorics is analogous to the Buckingham Π-theorem requirement that dimensionless predictions depend only on pure numbers. [PROVED]

13 CP Violation and the Jarlskog Invariant

Section summary. CP violation in three-generation mixing is measured by a convention-invariant quantity: the Jarlskog invariant. We define this invariant and then propose a simple, zero-parameter magnitude scale for CKM CP violation built from the same three CKM magnitudes already predicted in Sec. 3. The definition is mathematical ([PROVED]); the proposed structural magnitude and sign conventions are falsifiable hypotheses ([HYPOTHESIS]).

13.1 The Jarlskog invariant (definition and invariance)

For any 3×3 unitary mixing matrix W, the Jarlskog invariant can be written as a rephasing-invariant imaginary part of a 2×2 minor:

$$J(W) \;:=\; |\mathrm{Im}(W_{11}W_{22}W_{12}^{*}W_{21}^{*})| \,. \text{ [PROVED]} \tag{47}$$

The absolute value is included so that $J(W) \geq 0$ is a convention-independent magnitude. In the Standard Model, $J(V_{\text{CKM}}) \neq 0$ is the statement that quark mixing violates CP, while $J(U_{\text{PMNS}}) \neq 0$ is the analogous statement for leptons. [PROVED]

13.2 A minimal CKM CP scale from the ledger hierarchy

Section 3 proposes three CKM magnitudes with no per-channel tuning: $|V_{us}|_{\text{pred}}$, $|V_{cb}|_{\text{pred}}$, and $|V_{ub}|_{\text{pred}}$. [HYPOTHESIS]A minimal way to turn these into a CP-violation *scale* is to take their product:

$$J_{\text{CKM}}^{\text{pred}} \;:=\; |V_{us}|_{\text{pred}}\,|V_{cb}|_{\text{pred}}\,|V_{ub}|_{\text{pred}}. \text{ [HYPOTHESIS]} \tag{48}$$

Using the specific hypotheses of Sec. 3, this becomes the closed form

$$J_{\text{CKM}}^{\text{pred}} \;=\; \left(\varphi^{-3}\right)\left(\frac{1}{24}\right)\left(\frac{\alpha}{2}\right). \text{ [HYPOTHESIS]} \tag{49}$$

This proposal has two important features: (i) it introduces no new CP-specific fit parameters beyond the already-proposed mixing magnitudes, and (ii) it predicts the correct *order of magnitude* scale for CKM CP violation if the Sec. 3 magnitudes are correct. [HYPOTHESIS]

13.3 Sign conventions and falsifiers

Because $J(W)$ in Eq. (**??**) is a magnitude, it does not encode a sign. A sign can be attached only after fixing a generation ordering and phase convention; in this paper we reserve all such sign tests for the validation section. [CERT]

The falsifiers attached to this section are therefore magnitude-based: if the measured CKM Jarlskog invariant $J(V_{\mathrm{CKM}})$ is inconsistent with the predicted scale $J^{\mathrm{pred}}_{\mathrm{CKM}}$ in (**??**), then the "ledger-hierarchy" CP hypothesis is refuted. [VALIDATION]All numerical comparisons are carried out explicitly against PDG in Sec. 7. [VALIDATION]

Classical correspondence. The Jarlskog invariant $J(W)$ is mathematically identical to the standard SM rephasing-invariant measure of CP violation; the definition in Eq. (**??**) is the same as in the SM literature. The only structural addition is the proposal that $J^{\mathrm{pred}}_{\mathrm{CKM}}$ takes a closed form built from already-proposed mixing magnitudes, rather than being an independent fit parameter. This is a "Twin" correspondence: the mathematical object is the standard one, and the framework proposes its value rather than leaving it free. [PROVED]

14 Comparison to PDG and NuFIT

Section summary. This section validates the CKM/PMNS hypotheses of Secs. 3–6 against standard experimental summaries. All numerical targets are external (PDG for CKM, NuFIT for PMNS) and all agreement statements are labeled as validation ([VALIDATION]). No parameter is tuned per observable; in particular, the only small parameter is the shared constant α, and all integer coefficients are fixed by cube bookkeeping.

14.1 Reference targets and pinned constants

For CKM magnitudes and the quark-sector Jarlskog invariant we use the PDG summary values [**?**]. [VALIDATION]For PMNS mixing angles we use NuFIT 5.x summaries for normal ordering [**?**]. [VALIDATION]

For numerical evaluation of the closed forms, we pin the fine-structure constant for this section at

$$\alpha^{-1} := 137.036, \qquad \alpha := 1/\alpha^{-1}. \text{ [CERT]} \tag{50}$$

At the level of precision reported here, using nearby standard values of α does not change the qualitative conclusions. [CERT]

14.2 CKM magnitudes (validation)

The predicted magnitudes are those of Sec. 3, with the optional Cabibbo correction of Sec. 5:

$$|V_{cb}|_{\mathrm{pred}} = \frac{1}{24} \approx 0.04167, \text{ [VALIDATION]} \tag{51}$$

$$|V_{ub}|_{\mathrm{pred}} = \frac{\alpha}{2} \approx 0.00365, \text{ [VALIDATION]} \tag{52}$$

$$|V_{us}|_{\mathrm{pred}} = \varphi^{-3} \approx 0.23607, \text{ [VALIDATION]} \tag{53}$$

$$|V_{us}|_{\mathrm{pred,corr}} = \varphi^{-3} - \frac{3}{2}\alpha \approx 0.22512. \text{ [VALIDATION]} \tag{54}$$

Using representative PDG central values [**?**], $|V_{cb}|_{\rm ref} \approx 0.04182$, $|V_{ub}|_{\rm ref} \approx 0.00369$, $|V_{us}|_{\rm ref} \approx 0.22500$, the corresponding absolute discrepancies are

$$\big||V_{cb}|_{\rm pred} - |V_{cb}|_{\rm ref}\big| \approx 1.53 \times 10^{-4}, \text{ [VALIDATION]} \tag{55}$$

$$\big||V_{ub}|_{\rm pred} - |V_{ub}|_{\rm ref}\big| \approx 4.13 \times 10^{-5}, \text{ [VALIDATION]} \tag{56}$$

$$\big||V_{us}|_{\rm pred} - |V_{us}|_{\rm ref}\big| \approx 1.11 \times 10^{-2}, \text{ [VALIDATION]} \tag{57}$$

$$\big||V_{us}|_{\rm pred,corr} - |V_{us}|_{\rm ref}\big| \approx 1.22 \times 10^{-4}. \text{ [VALIDATION]} \tag{58}$$

Thus, the corrected Cabibbo hypothesis Eq. (**??**) is strongly preferred over the leading-order φ^{-3} value when judged against PDG. [VALIDATION]

14.3 CKM CP violation scale (validation)

Section 6 proposes the CKM CP scale $J^{\rm pred}_{\rm CKM} := |V_{us}|\ |V_{cb}|\ |V_{ub}|$ (no additional parameters). [HYPOTHESIS]Evaluating the closed form Eq. (**??**) gives

$$J^{\rm pred}_{\rm CKM} \approx 3.59 \times 10^{-5}. \text{ [VALIDATION]} \tag{59}$$

If one instead uses the corrected Cabibbo variant $|V_{us}|_{\rm pred,corr}$ in the product (still no new knobs), one obtains

$$J^{\rm pred,corr}_{\rm CKM} := |V_{us}|_{\rm pred,corr}\ |V_{cb}|_{\rm pred}\ |V_{ub}|_{\rm pred} \approx 3.42 \times 10^{-5}. \text{ [VALIDATION]} \tag{60}$$

For comparison, PDG reports a quark-sector Jarlskog magnitude $J^{\rm ref}_{\rm CKM} \sim 3.1{\times}10^{-5}$ [**?**]. [VALIDATION]

14.4 PMNS mixing angles (validation and current tension)

The PMNS hypotheses of Sec. 4 evaluate (with the pinned α) to

$$\sin^2\theta^{\rm pred}_{13} \approx 0.02129, \text{ [VALIDATION]} \tag{61}$$

$$\sin^2\theta^{\rm pred}_{12} \approx 0.30899, \text{ [VALIDATION]} \tag{62}$$

$$\sin^2\theta^{\rm pred}_{23} \approx 0.54378. \text{ [VALIDATION]} \tag{63}$$

Using NuFIT 5.x (normal ordering) as a standard experimental summary [**?**], two points are immediate:

- **Reactor and solar angles.** $\sin^2\theta_{13}$ and $\sin^2\theta_{12}$ are in reasonable agreement with NuFIT best-fit values at the level of current uncertainties (validation). [VALIDATION]
- **Atmospheric angle and octant.** The hypothesis $\sin^2\theta^{\rm pred}_{23} = 1/2 + 6\alpha$ implies an *upper-octant* value. NuFIT continues to show octant sensitivity, and current fits may place the best fit away from the predicted point; this is an active tension and therefore a near-term falsifier. [VALIDATION]

14.5 Referee checklist for any comparison

Any objection or alternative comparison should specify:

- the target summary (PDG vs a specific global-fit release),

- the target parameterization (e.g. whether $\sin^2\theta_{ij}$ or θ_{ij} is being reported),
- for PMNS, the ordering and the octant convention being assumed,
- and the exact hypothesis being tested (leading-order vs corrected Cabibbo; which PMNS correction terms are included).

15 The Deep Ladder: Fractional Rungs

Section summary. We define the ladder coordinate used for neutrinos and introduce the "deep" regime where rungs are taken to be fractional. The ladder mathematics is elementary ([PROVED]); the physical claim is the fractional-rung assignment and its specific step size ([HYPOTHESIS]). This section fixes notation so that later sections can state masses and splittings without hidden fitting knobs.

15.1 Ladder coordinate and rungs

As in Papers 1–2, we encode multiplicative hierarchy by a base-φ scale coordinate. For a positive quantity x, define its ladder coordinate by

$$r(x) \;:=\; \log_\varphi(x). \text{ [PROVED]} \tag{64}$$

Equivalently, specifying a rung r specifies a pure ladder factor φ^r. [PROVED]

In the charged sectors we treated rungs as integers. For neutrinos we extend the rung set to rationals:

$$r \in \tfrac{1}{4}\mathbb{Z}. \text{ [HYPOTHESIS]} \tag{65}$$

Equation (**??**) is a convention for the deep ladder: it asserts that the relevant rung lattice is a quarter-step lattice. No numerical value is being fit here; the claim is that neutrinos exhibit a finer rung resolution than the charged sectors. [HYPOTHESIS]

15.2 Why quarter steps (motivation, not a fit)

The quarter-step convention is motivated by two qualitative constraints:

- **Resolution.** Neutrino splittings are extremely small compared to charged sectors, suggesting that the deep ladder must resolve much smaller exponent increments than integer rungs provide. [HYPOTHESIS]
- **Compatibility with the octave clock.** The series uses an eight-tick closure as a canonical cycle; quarter rungs provide a simple compatible refinement that is still discrete and auditable. [HYPOTHESIS]

These motivations are not proofs; the quarter-step lattice is judged by falsifiers (Sec. 8). [VALIDATION]

15.3 Rung differences and squared-mass ratios

A key reason to use a ladder coordinate is that ratios become differences. If two masses $m_a, m_b > 0$ differ by rung offset $\Delta r := r(m_a) - r(m_b)$, then

$$\frac{m_a}{m_b} = \varphi^{\Delta r}. \text{ [PROVED]} \tag{66}$$

For squared masses this becomes

$$\frac{m_a^2}{m_b^2} = \varphi^{2\Delta r}. \text{ [PROVED]} \tag{67}$$

Later, the neutrino rung assignments will imply a rigid φ-power ratio for the atmospheric-to-solar splitting scale. [PROVED]

15.4 Rung assignment (to be used in later sections)

We denote the three neutrino rungs by $r_1 < r_2 < r_3$ (normal ordering). [HYPOTHESIS]In later sections we will use the specific deep-ladder assignment

$$(r_1, r_2, r_3) := \left(-\frac{239}{4}, -\frac{231}{4}, -\frac{217}{4}\right). \text{ [HYPOTHESIS]} \tag{68}$$

Equation (**??**) is the core discrete input for the neutrino sector in this paper. It is not tuned per mass eigenstate; it is a single rung triple whose consequences are then checked against external oscillation summaries. [HYPOTHESIS]

Classical correspondence. The logarithmic ladder coordinate $r(x) = \log_\varphi(x)$ is a standard change of variables; what is novel is the fractional-rung lattice $r \in \frac{1}{4}\mathbb{Z}$. There is no direct classical analog to discrete quarter-step rungs: in continuum field theory, masses vary continuously. The closest conceptual relative is a discrete quantum number (like spin projection or isospin component) that restricts allowed states to a lattice. The compatibility of quarter steps with the eight-tick octave ($8 \times \frac{1}{4} = 2$) is an internal consistency check, analogous to requiring that lattice refinements divide evenly into fundamental periods (T6 bridge). [HYPOTHESIS]

16 Neutrino Mass Predictions

Section summary. Given a discrete rung triple (r_1, r_2, r_3) and a single global calibration seam for eV reporting, the deep ladder yields three absolute neutrino masses. The rung triple is the only neutrino-sector discrete input ([HYPOTHESIS]); the eV scale is fixed once for the overall framework ([CERT]); the numerical values quoted here are the consequence of those declarations (and are later compared to external constraints as validation).

16.1 From rungs to eV masses (explicit reporting seam)

Section 2 fixes the neutrino rung triple $(r_1, r_2, r_3) \in (\frac{1}{4}\mathbb{Z})^3$ (Eq. (**??**)). [HYPOTHESIS]To report absolute masses in eV, we require a declared calibration seam that converts one ladder "coherence quantum" to SI energy. We represent that seam by a single scalar τ_0 (seconds per ladder tick), and define the corresponding eV scale

$$\kappa_{\mathrm{eV}} := \frac{\hbar}{\tau_0} \Big/ (1\,\mathrm{eV}). \text{ [CERT]} \tag{69}$$

This seam is global: it is fixed once for the framework and is not adjusted per neutrino eigenstate. [CERT]

With κ_{eV} fixed, the deep-ladder mass hypothesis is:

$$m_i^{\mathrm{pred}} := \kappa_{\mathrm{eV}}\, \varphi^{r_i}, \qquad i \in \{1, 2, 3\}. \text{ [HYPOTHESIS]} \tag{70}$$

16.2 Predicted absolute masses (numerical evaluation under the seam)

Evaluating Eq. (**??**) for the rung triple (**??**) under the declared seam yields the absolute mass window:

$$0.00352 < m_1^{\mathrm{pred}} < 0.00355 \text{ eV}, \text{ [CERT]} \tag{71}$$

$$0.00924 < m_2^{\mathrm{pred}} < 0.00928 \text{ eV}, \text{ [CERT]} \tag{72}$$

$$0.04987 < m_3^{\mathrm{pred}} < 0.04993 \text{ eV}. \text{ [CERT]} \tag{73}$$

The implied mass sum is therefore

$$0.06263 < \sum_{i=1}^{3} m_i^{\mathrm{pred}} < 0.06276 \text{ eV}. \text{ [CERT]} \tag{74}$$

Compatibility with cosmological and kinematic constraints is assessed later as validation, not used to set τ_0 or the rungs. [VALIDATION]

Classical correspondence. The mass prediction $m_i^{\mathrm{pred}} = \kappa_{\mathrm{eV}}\,\varphi^{r_i}$ is an instance of the single-anchor mass law used throughout the series: a global scale factor times a pure φ-power determined by a discrete rung. This corresponds to the phenomenological "quantum ladder" structure observed in many hierarchical mass spectra, where ratios between adjacent states follow a geometric progression. The calibration seam κ_{eV} plays the role of an overall unit conversion (Bridge to SI), analogous to fixing $\hbar$ or c when reporting energies in eV rather than inverse seconds. No per-eigenstate fitting is introduced; the entire mass hierarchy is encoded in the rung triple. [HYPOTHESIS]

17 Mass-Squared Splittings

Section summary. Oscillation experiments measure mass-squared splittings rather than absolute masses. Given the deep-ladder masses from Sec. 3, we define the two independent splittings and evaluate them under the declared eV reporting seam. The resulting values are then compared to NuFIT summary windows as validation.

17.1 Definitions

We use the standard definitions (normal ordering conventions are discussed later):

$$\Delta m^2_{21} \;:=\; m_2^2 - m_1^2, \qquad \Delta m^2_{31} \;:=\; m_3^2 - m_1^2. \text{ [PROVED]} \tag{75}$$

If $m_1 < m_2 < m_3$ (normal ordering), then both splittings are positive. [PROVED]

17.2 Predicted splittings from the deep ladder

Using the mass law of Sec. 3, Eq. (**??**), the predicted splittings are

$$\Delta m^{2\,\mathrm{pred}}_{ij} \;=\; \left(m_i^{\mathrm{pred}}\right)^2 - \left(m_j^{\mathrm{pred}}\right)^2 \;=\; \kappa_{\mathrm{eV}}^2\left(\varphi^{2r_i} - \varphi^{2r_j}\right). \text{ [PROVED]} \tag{76}$$

Thus, while the absolute eV-scale splittings depend on the global seam parameter κ_{eV}, the *ratio* of splittings depends only on rung differences:

$$\frac{\Delta m^{2\,\mathrm{pred}}_{31}}{\Delta m^{2\,\mathrm{pred}}_{21}} \;=\; \frac{\varphi^{2r_3} - \varphi^{2r_1}}{\varphi^{2r_2} - \varphi^{2r_1}}. \text{ [PROVED]} \tag{77}$$

The next section derives the exact φ-power relation $(m_3^{\rm pred})^2/(m_2^{\rm pred})^2 = \varphi^7$ implied by the deep rung spacing, and records the resulting closed-form (seam-free) prediction for the splitting ratio as a fixed function of φ. [HYPOTHESIS]

17.3 Numerical evaluation and validation

Evaluating the splittings using the mass bounds from Sec. 3 (Eq. (**??**)) yields the representative values

$$\Delta m^2_{21}{}^{\rm pred} \approx 7.33 \times 10^{-5}\ {\rm eV}^2, \text{ [CERT]} \tag{78}$$

$$\Delta m^2_{31}{}^{\rm pred} \approx 2.48 \times 10^{-3}\ {\rm eV}^2. \text{ [CERT]} \tag{79}$$

As a validation check, we compare to NuFIT 5.x summary windows for normal ordering [**?**]. At the level of precision used in this paper, the predictions satisfy:

$$7.21 \times 10^{-5} < \Delta m^2_{21}{}^{\rm pred} < 7.62 \times 10^{-5}\ {\rm eV}^2, \text{ [VALIDATION]} \tag{80}$$

$$2.455 \times 10^{-3} < \Delta m^2_{31}{}^{\rm pred} < 2.567 \times 10^{-3}\ {\rm eV}^2. \text{ [VALIDATION]} \tag{81}$$

These comparisons are strictly validation: the NuFIT windows are not used to set the rungs or the calibration seam. [VALIDATION]

Classical correspondence. The mass-squared splittings Δm^2_{21} and Δm^2_{31} are mathematically identical to the standard oscillation observables used in NuFIT and PDG summaries (Twin status). The key structural addition is Eq. (**??**): the *ratio* of splittings is seam-free because the global scale $\kappa^2_{\rm eV}$ cancels. This mirrors how mass-ratio predictions in QFT are often more robust than absolute-scale predictions, since renormalization-scale dependence cancels in ratios. The framework predicts concrete numerical values for both splittings (Bridge to oscillation phenomenology), but the falsifiable core is the seam-free ratio. [HYPOTHESIS]

18 The φ^7 Ratio

Section summary. The deep rung spacing implies an *exact* φ-power relation among the neutrino squared masses. This exact ratio is independent of the eV calibration seam. We also record the induced (seam-free) closed form for the ratio of the measured mass-squared splittings.

18.1 An exact squared-mass ratio from rung differences

From the mass law $m_i^{\rm pred} = \kappa_{\rm eV}\varphi^{r_i}$ (Eq. (**??**)), the seam cancels in squared-mass ratios:

$$\frac{\left(m_3^{\rm pred}\right)^2}{\left(m_2^{\rm pred}\right)^2} \;=\; \frac{\kappa^2_{\rm eV}\varphi^{2r_3}}{\kappa^2_{\rm eV}\varphi^{2r_2}} \;=\; \varphi^{2(r_3-r_2)}. \text{ [PROVED]} \tag{82}$$

Under the specific deep rung assignment of Eq. (**??**), the rung gap is

$$r_3 - r_2 = \frac{7}{2}. \text{ [HYPOTHESIS]} \tag{83}$$

Substituting (**??**) into (**??**) yields the advertised exact ratio:

$$\frac{\left(m_3^{\rm pred}\right)^2}{\left(m_2^{\rm pred}\right)^2} \;=\; \varphi^7. \text{ [HYPOTHESIS]} \tag{84}$$

Equivalently, $m_3^{\rm pred}/m_2^{\rm pred} = \varphi^{7/2}$. [HYPOTHESIS]

18.2 Induced prediction for the splitting ratio (seam-free)

While the squared-mass ratio is a pure φ-power, the *splitting* ratio depends on m_1 as well. Using Eq. (**??**) together with the rung differences from Eq. (**??**): $r_2 - r_1 = 2$ and $r_3 - r_1 = 11/2$, one obtains the closed form

$$\frac{\Delta m^2_{31}{}^{\rm pred}}{\Delta m^2_{21}{}^{\rm pred}} \;=\; \frac{\varphi^{11}-1}{\varphi^4-1} \;\approx\; 33.823. \text{ [HYPOTHESIS]} \tag{85}$$

This ratio is *seam-free*: it depends only on the discrete rung differences and on φ, not on $\kappa_{\rm eV}$. [PROVED]Its agreement with experimental summaries is assessed as validation (Sec. 4 and Sec. 8). [VALIDATION]

Classical correspondence. The exact relation $(m_3^{\rm pred})^2/(m_2^{\rm pred})^2 = \varphi^7$ is the neutrino-sector analog of the mass-family-ratio predictions in Paper 1: when two species share the same ladder base, their mass ratio is a pure φ-power determined by the rung difference. This corresponds to the general phenomenological observation that hierarchical mass spectra often exhibit geometric-progression structure (Bridge to Yukawa texture models). The crucial feature is that the seam cancels: the ratio is a dimensionless, convention-free prediction testable by oscillation experiments alone. This is the falsifiable core of the deep-ladder hypothesis. [HYPOTHESIS]

19 Normal Hierarchy from Geometry

Section summary. The ordering of neutrino masses (normal vs inverted) is an experimental question, but in the deep-ladder framework the ordering is not an independent fit knob: it is fixed by the rung ordering together with monotonicity of the φ-ladder map. We record this implication explicitly and state what would falsify it.

19.1 Monotonicity of the ladder map

The ladder base satisfies $\varphi > 1$. [PROVED]For any fixed $\kappa_{\rm eV} > 0$, the mapping

$$r \mapsto m(r) := \kappa_{\rm eV}\, \varphi^r \text{ [PROVED]} \tag{86}$$

is strictly increasing in r. [PROVED]Therefore rung ordering implies mass ordering. [PROVED]

19.2 Normal ordering implied by the deep rungs

Section 2 fixes the neutrino rungs (r_1, r_2, r_3) with

$$r_1 < r_2 < r_3. \text{ [HYPOTHESIS]} \tag{87}$$

Combining Eq. (**??**) with the monotonicity of Eq. (**??**) yields

$$m_1^{\text{pred}} < m_2^{\text{pred}} < m_3^{\text{pred}}. \text{ [PROVED]} \tag{88}$$

Thus, within this framework, "normal ordering" is not a choice made to match an external fit; it is the direct consequence of the discrete rung assignment. [HYPOTHESIS]

19.3 Validation and falsifier

Global oscillation analyses currently favor normal ordering, but the ordering remains an experimental output rather than an input to this paper. [VALIDATION]If future oscillation and matter-effect measurements decisively establish inverted ordering, then the deep rung hypothesis (and in particular the rung triple of Eq. (**??**)) is refuted. [VALIDATION]

Classical correspondence. The statement "rung ordering implies mass ordering" has no direct classical analog: in continuum field theory, mass eigenvalues can be permuted freely by relabeling. The closest conceptual relative is the constraint that quantum numbers (e.g. principal quantum number in atomic physics) order energy levels. Here the rung triple is a discrete topological input (T9), and the monotonicity of φ^r enforces a rigid mass ordering without additional fitting. This is a *Novel* structural claim: the ordering is not a choice but a consequence of the deep-ladder assignment. [HYPOTHESIS]

20 Cosmological Constraints

Section summary. Cosmological data constrain neutrino masses primarily through the sum $\sum m_\nu$. In the deep-ladder framework, $\sum m_\nu$ is predicted once the rung triple and the global eV reporting seam are fixed. Cosmological bounds are model-dependent and are used only for validation, never as an input.

20.1 What cosmology constrains

In standard cosmological analyses, the leading sensitivity to neutrino masses is through the total mass sum

$$\Sigma_\nu \;:=\; m_1 + m_2 + m_3. \text{ [PROVED]} \tag{89}$$

The exact numerical bound on Σ_ν depends on the assumed cosmological model (e.g. ΛCDM vs extensions) and the datasets included. For this reason, we treat cosmological constraints strictly as validation checks rather than as part of the model layer. [VALIDATION]

20.2 Deep-ladder prediction for the mass sum

Section 3 derived the predicted mass-sum window under the declared eV seam:

$$0.06263 < \Sigma_\nu^{\text{pred}} < 0.06276 \text{ eV}. \text{ [CERT]} \tag{90}$$

This value is not obtained by fitting cosmological data; it is implied by the rung triple and the single global reporting seam. [CERT]

20.3 Validation against current cosmological bounds

The Particle Data Group summarizes cosmological limits on Σ_ν and emphasizes their model dependence [**?**]. [VALIDATION]Using representative current bounds (typically at the $\Sigma_\nu \lesssim 0.12\,\mathrm{eV}$ level in ΛCDM-like analyses), the predicted range (**??**) is comfortably allowed. [VALIDATION]Future tightening of cosmological bounds toward $\Sigma_\nu < 0.06\,\mathrm{eV}$ would directly pressure or refute the deep-ladder mass scale. [VALIDATION]

21 Falsifiers

This section lists experimental outcomes that would refute the deep-ladder hypothesis class proposed in this paper. We distinguish *seam-free* falsifiers (independent of the eV calibration seam) from *scale* falsifiers (which test the declared eV reporting seam). [PROVED]

21.1 Seam-free falsifiers (depend only on rung differences and φ)

F1: splitting-ratio mismatch. Define the experimentally inferred splitting ratio

$$R_\Delta \;:=\; \frac{\Delta m^2_{31}}{\Delta m^2_{21}}. \text{ [PROVED]} \tag{91}$$

Under the rung triple of Eq. (**??**), the model predicts the seam-free value

$$R_\Delta^{\mathrm{pred}} \;=\; \frac{\varphi^{11}-1}{\varphi^4-1} \;\approx\; 33.823. \text{ [HYPOTHESIS]} \tag{92}$$

This hypothesis is falsified if the best-fit R_Δ inferred from oscillation data (for the stated ordering and dataset release) becomes inconsistent with R_Δ^{pred} beyond the quoted experimental uncertainty. [VALIDATION]

F2: ordering mismatch. The deep rungs are ordered $r_1 < r_2 < r_3$ (Eq. (**??**)), which implies normal mass ordering $m_1 < m_2 < m_3$ (Eq. (**??**)). [HYPOTHESIS]If future oscillation and matter-effect measurements decisively establish inverted ordering, the rung triple hypothesis is refuted. [VALIDATION]

F3: squared-mass ratio mismatch (requires absolute-mass information). The rung gap $r_3 - r_2 = 7/2$ implies the exact squared-mass ratio $(m_3^{\mathrm{pred}})^2/(m_2^{\mathrm{pred}})^2 = \varphi^7$ (Eq. (**??**)). [HYPOTHESIS]If future absolute-mass information (together with ordering identification) determines m_3^2/m_2^2 in a way that excludes φ^7, this rung-gap hypothesis is refuted. [VALIDATION]

21.2 Scale falsifiers (test the declared eV reporting seam)

F4: exclusion by oscillation windows for Δm^2. The deep ladder predicts specific eV-scale splittings (Sec. 4) once the global seam is fixed. [CERT]If updated NuFIT (or successor) summary windows for the stated ordering exclude ${\Delta m^2_{21}}^{\mathrm{pred}}$ or ${\Delta m^2_{31}}^{\mathrm{pred}}$ at high significance, then either the rung triple or the declared eV seam is refuted. [VALIDATION]

F5: cosmological exclusion of Σ_ν. The predicted mass sum is $\Sigma_\nu^{\mathrm{pred}} \approx 0.0627\,\mathrm{eV}$ (Eq. (**??**)). [CERT]If cosmological analyses (under clearly stated model assumptions) establish an upper bound $\Sigma_\nu < 0.0626\,\mathrm{eV}$, then the deep-ladder mass scale is ruled out. [VALIDATION]

F6: direct absolute-mass detection above the predicted scale. Any direct kinematic or laboratory measurement that robustly implies a neutrino mass scale well above the predicted window of Eq. (**??**) (under the same declared reporting seam) refutes the deep-ladder mass assignment. [VALIDATION]

22 Interaction Bridge: EFT Matching at the Anchor

Section summary. The framework presented so far predicts particle masses (m) as structural geometric data. Standard Model (SM) predictions for interaction rates (cross-sections, decay widths) are typically parameterized by Yukawa couplings (y_f). This section defines the bridge: we treat the SM as an effective field theory (EFT) and *match* the Yukawa couplings at the anchor scale $\mu_\star$ to reproduce the structural masses. This procedure allows standard QFT calculation of interaction rates without introducing new free parameters.

22.1 The status of Yukawa couplings in this framework

In the Standard Model, the Yukawa coupling y_f is a free parameter that simultaneously determines the mass (m_f) and the interaction strength with the Higgs boson ($g_{f\bar{f}H}$). In the present framework, the mass $m_f(\mu_\star)$ is a derived structural quantity (determined by the sector yardstick, rung r, and band Z).

Consequently, the Yukawa coupling is not treated as a fundamental degree of freedom. Instead, it is a **dependent effective parameter** derived by matching the SM description to the structural mass at the anchor scale.

22.2 Matching definition at $\mu_\star$

We define the effective Yukawa coupling $y_f(\mu_\star)$ in the $\overline{\text{MS}}$ scheme by the matching condition:

$$y_f(\mu_\star) \;:=\; \frac{\sqrt{2}\, m_f^{\text{struct}}(\mu_\star)}{v(\mu_\star)}. \tag{93}$$

Here:

- $m_f^{\text{struct}}(\mu_\star)$ is the mass predicted by the structural laws (Eqs. (**??**), (**??**), etc.). [PROVED]
- $v(\mu_\star)$ is the Standard Model vacuum expectation value evaluated at the anchor scale. For consistency, v is fixed by the Fermi constant G_F (extracted from muon decay) via the standard relation $v = (\sqrt{2}G_F)^{-1/2} \approx 246.22$ GeV. [CERT]

This definition ensures that the "inertia" (mass) and "interaction" (coupling) remain consistent with the SM gauge symmetries, while reducing the number of free inputs in the theory.

22.3 Calculation of interaction rates (Higgs decay)

Once the effective Yukawa $y_f(\mu_\star)$ is fixed by the matching condition, interaction observables are calculated using standard perturbative QFT.

For example, the partial decay width of the Higgs boson to fermions, $H \to f\bar{f}$, is given at leading order by:

$$\Gamma(H \to f\bar{f}) \;=\; \frac{N_c G_F}{4\pi\sqrt{2}}\, m_f^2(\mu_H)\, M_H \left(1 - \frac{4m_f^2}{M_H^2}\right)^{3/2}, \tag{94}$$

where $m_f(\mu_H)$ is the running mass evaluated at the Higgs mass scale $\mu_H \approx 125$ GeV.

Transport hygiene. To evaluate this rate, one must transport the structural mass from the anchor $\mu_\star$ to the Higgs scale μ_H. As defined in the transport policy (Sec. 7), this is a bookkeeping step using the SM beta functions:

$$m_f(\mu_H) \;=\; m_f^{\mathrm{struct}}(\mu_\star) \cdot \exp\left(- \int_{\ln \mu_\star}^{\ln \mu_H} \gamma_m(\mu)\, d\ln \mu \right). \text{[CERT]} \tag{95}$$

Thus, the framework predicts interaction rates with no adjustable parameters beyond the declared transport policy.

22.4 Falsifiability via interaction deviations

This matching procedure assumes that the SM relation between mass and interaction strength ($g \propto m$) holds exactly. Any deviation from this relation (e.g., anomalous Higgs couplings) would indicate new physics beyond the structural mass generation described here. Current LHC measurements of Higgs couplings are consistent with the SM predictions (and therefore with this matching procedure) within uncertainties. Future precision measurements of $H \to \mu\mu$ and $H \to \tau\tau$ will serve as critical tests of whether the geometric rung structure correctly encodes the interaction vertex strength. [VALIDATION]

23 Unified Falsifiers and Conclusions

The framework presented here is maximally falsifiable. It replaces continuous free parameters with discrete integer choices. If the predicted correlations (e.g., the φ^7 neutrino ratio, or the equal-Z clustering at $\mu_\star$) are violated by future precision data, the specific structural hypotheses are refuted.

23.1 Summary of key falsifiers

1. **Charged Lepton Precision:** The electron-muon-tau ladder must hold to within RG transport uncertainties.
2. **Neutrino Splitting Ratio:** The ratio $\Delta m^2_{31}/\Delta m^2_{21}$ is predicted to be ≈ 33.8 (seam-free).
3. **PMNS Octant:** The atmospheric angle θ_{23} is predicted to be in the upper octant ($\sin^2\theta_{23} > 0.5$).
4. **Interaction Rates:** Higgs branching ratios must be consistent with the Yukawa couplings derived from the geometric masses.

A Reproducibility and Data

All numerical results in this paper are reproducible from the associated code repository. Transport policies and calibration seams are explicitly declared in the supplementary material.

References

[1] Particle Data Group, *Review of Particle Physics* (2024 edition).

[2] NuFIT Collaboration, *Neutrino oscillation global fit results* (NuFIT 5.x).

[3] CODATA, *Recommended values of the fundamental physical constants* (latest release used in comparisons).